

The performance of the free-standing P(VDF-TrFE) infrared detector

TIAN Li¹, SUN Jing-Lan², WANG Jian-Lu², MENG Xiang-Jian², CHU Jun-Hao²

(1. College of Electrical and Information Engineering, Hunan Institute of Engineering, Xiangtan 411101, China;

2. National Laboratory of Infrared Physics, Shanghai Institute of Technical Physics,
Chinese Academy of Sciences, Shanghai 200083, China)

Abstract: Free-standing infrared detector with an Al/P(VDF-TrFE)/NiCr structure was fabricated. A semitransparent NiCr metal thin film on top of the device served as both electrode and absorption layer. The experimental results reveal that P(VDF-TrFE) has good ferroelectric and pyroelectric properties with remanent polarization $7.1 \mu\text{C}/\text{cm}^2$ and pyroelectric coefficient $27 \mu\text{C}/\text{m}^2\text{K}$ respectively. The voltage responsivity R_V and detectivity D^* of the device at 10 Hz with blackbody source temperature at 500 K are around 1 500 V/W and $5 \times 10^7 \text{cmHz}^{1/2}\text{W}^{-1}$, respectively. The thermal conductance of unit area to the environment and absorption of the detector were estimated to be $2.5 \times 10^{-3} \text{W}/\text{cm}^2\text{K}$ and 0.1, respectively, from the frequency dependence of the voltage responsivity. Using the detector, the thermal image of target was obtained.

Key words: P(VDF-TrFE) film, voltage responsivity, infrared detector

PACS: 77.55.kt

自支撑 P(VDF-TrFE) 红外探测器

田莉¹, 孙璟兰², 王建禄², 孟祥建², 褚君浩²

(1 湖南工程学院 电气信息学院, 湖南湘潭 411101;

2. 中国科学院上海技术物理研究所 红外物理国家重点实验室, 上海 200083)

摘要: 制备了具有自支撑绝热结构的 Al/P(VDF-TrFE)/NiCr 红外探测器单元, 其中 NiCr 半透明膜作为探测器的上电极和吸收层。实验结果表明: P(VDF-TrFE) 薄膜具有很好的铁电性和热释电性, 其铁电剩余极化强度和热释电系数分别为 $7.1 \mu\text{C}/\text{cm}^2$ 和 $27 \mu\text{C}/\text{m}^2\text{K}$; 探测器单元在 10 Hz 工作频率下对黑体温度 500 K 的辐射源的电压响应率和探测率分别为 1 500 V/W 和 $5 \times 10^7 \text{cmHz}^{1/2}\text{W}^{-1}$; 通过对电压响应率随频率变化的实验数据进行拟合, 得到探测器单位面积的热导和吸收率分别为 $2.5 \times 10^{-3} \text{W}/\text{cm}^2\text{K}$ 和 0.1; 利用 P(VDF-TrFE) 探测器单元可对目标物体实现热成像。

关键词: P(VDF-TrFE) 薄膜; 电压响应率; 红外探测器

中图分类号: TN215 文献标识码: A

Introduction

During the last several decades interests in developing uncooled infrared (IR) detectors have continuously increased^[1-4]. Among the ferroelectric materials available, poly(vinylidene fluoride trifluoroethylene) [P(VDF-TrFE)] copolymer becomes the subject of intense research for uncooled IR detectors because of relatively high pyroelectric coefficient, low processing temperature,

easy processing on large substrate, excellent flexibility, mechanical resistance and low cost^[5]. It is expected that the P(VDF-TrFE) detectors will have wide applications in thermal imaging, night vision and surveillance.

In our previous studies, IR detectors with polyimide/Al/P(VDF-TrFE)/Al structure were studied^[6]. In this structure, the top metal Al serves as both electrode and absorbing layer. Although good performance were obtained, optimization of the detector design was very necessary to improve their performance. For optimization

Received date: 2014-11-19, **revised date:** 2015-09-22

收稿日期: 2014-11-19, **修回日期:** 2015-09-22

Foundation items: Supported by Scientific Research Fund of Hunan Provincial Education Department (14B041), the Natural Science Foundation of Hunan Province (2015JJ6024, 14JJ6040), National Natural Science Foundation of China(51502087)

Biography: TIAN Li (1980-), female, Hunan, China, Postgraduate. Research fields focus on infrared detector. E-mail: tianli5222003@aliyun.com

of the detector design, several aspects must be considered^[7]. Firstly, the heat capacity of the total arrangement of the detector has to be small to decrease the thermal time constant of the device. To do this, we can peel the sensor off the polyimide substrate by oxygen ion etching to form free-standing detectors. Secondly, the absorption for incoming radiation can be improved. It has been reported that NiCr film with impedance matched to that of incident infrared radiation can absorb 50% of IR radiation^[8]. Thus, in this work free-standing detectors with Al/P(VDF-TrFE)/NiCr structure were fabricated. The ferroelectric, pyroelectric properties and performance of the detector were studied. Besides, the performance of free-standing detectors with Al/P(VDF-TrFE)/Al structure was also studied for comparison.

1 Experimental details

The detector structure is Al/P(VDF-TrFE)/NiCr. Al stripes of 120 nm thick and 0.3 mm wide were first evaporated on the polyimide substrate as the bottom electrode. P(VDF-TrFE) thin films with the composition of 70/30 mol% were prepared on Al electrodes by the spin-coating method^[9]. The total P(VDF-TrFE) films are about 500 nm. Then 0.2 mm wide NiCr stripes, which serve as both top electrode and absorption layer, were fabricated onto the films to form an Al/polymer/NiCr structure. Finally, we peeled the sensors off the polyimide by oxygen ion etching to form free-standing detectors. As a comparison, free-standing Al/P(VDF-TrFE)/Al samples were also fabricated according to the processes mentioned above.

The crystal structure of the samples was analyzed by the standard x-ray diffraction (Bruker Advanced diffractometer). The polarization versus electric field (P - E) hysteresis loops were measured using a Radiant Precision LC system. The dielectric properties were measured using a HP4194A impedance/gain analyzer with an ac drive voltage of 0.02 V. The pyroelectric property was characterized by monitoring the dynamic pyroelectric current while the temperature of the sample is modulated periodically^[10]. The voltage response of the detector to the IR radiation was measured with blackbody source temperature at 500 K and an optical chopper working at the range of 2 Hz to 80 Hz. All the measurement were carried out in ambient atmosphere.

2 Results and discussion

Figure 1 shows the XRD patterns for P(VDF-TrFE) film grown on Al. One diffraction peak was observed, which was assigned to the typical (110) and/or (200) of the ferroelectric β phase of P(VDF-TrFE)^[11]. Because of the pseudo-hexagonal symmetry of the crystal normal to the polymer chain direction, (110) and (200) reflections overlap and cannot be resolved. Inset figure shows the polarization-electric field (P - E) loops for Al/P(VDF-TrFE)/NiCr samples. It is shown that well saturated P - E hysteresis loops are obtained, indicating P(VDF-TrFE) good ferroelectricity. The magnitude of the P_r is about $7.1 \mu\text{C}/\text{cm}^2$.

Prior to the measurement of the pyroelectric

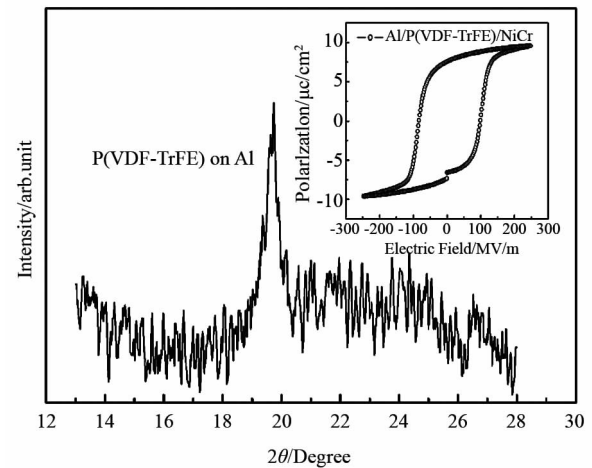


Fig.1 XRD pattern for P(VDF-TrFE) film on Al, inset is the P - E loop for P(VDF-TrFE) film

图1 生长在金属 Al 上的 P(VDF-TrFE) 薄膜的 XRD 图, 插图图为 P(VDF-TrFE) 薄膜的电滞回线

coefficient, the samples were sufficiently poled. The sample temperature was modulated sinusoidally at a frequency of 0.045 Hz while the pyroelectric current was recorded by an electrometer. The measured pyroelectric coefficient of P(VDF-TrFE) is $27 \mu\text{C}/\text{m}^2\text{K}$.

To evaluate the performance of the detectors, the voltage response of the detector was measured. Figure 2 shows the voltage responses to modulated IR radiation at 2 Hz. The frequency dependence of voltage responsivity R_V , noise and specific detectivity of the sample are shown in Fig. 3. The voltage responsivity at 10 Hz is $1500 \text{ V}/\text{W}$, which is much bigger than our previous value of $209 \text{ V}/\text{W}$ in polyimide/Al/P(VDF-TrFE)/Al detectors. As a comparison, the voltage responsivity of the later is also shown in Fig. 3.

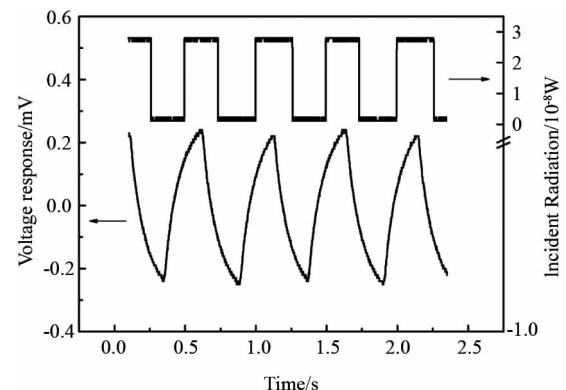


Fig.2 Voltage response to the modulated incident radiation at 2 Hz

图2 调制频率为 2 Hz 时器件的电压响应

To obtain thermal time constant τ_T and absorption coefficient η , the basic character parameters of the sample respectively, the frequency dependence of the voltage responsivity in Fig. 3 for the two kinds of samples is simulated using the following equations^[7]

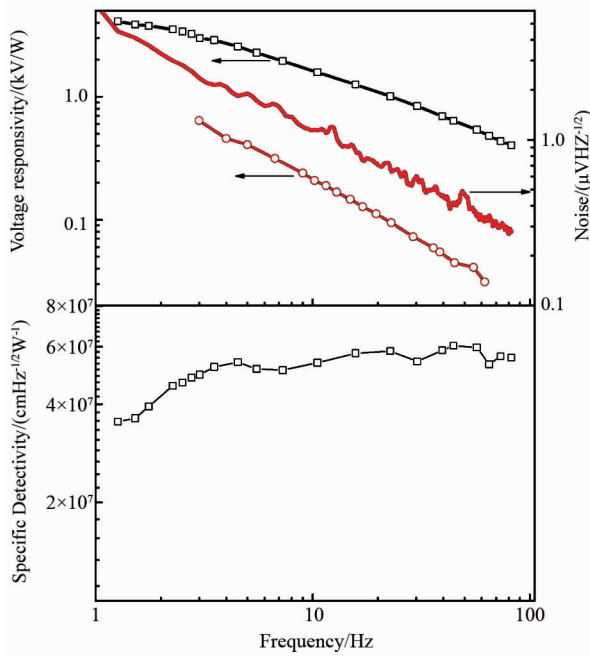


Fig. 3 The frequency dependence of voltage responsivity and noise represented by square dots and line, respectively (upper panel), and specific detectivity of detectors (lower panel). As a comparison, the voltage responsivity of Al/P(VDF-TrFE)/Al is also shown by circle dots in the upper panel.

图3 探测器电压响应率,噪声和探测率随调制频率的变化.上图中方块代表电压响应率,实线为噪声,下图为从电压响应率和噪声计算得到的探测率.作为对比,Al/P(VDF-TrFE)/Al器件的电压响应率也在上图中给出,数据用圆圈表示

$$R_v = \frac{\eta p}{k_T C} \frac{1}{(1 + (\omega \tau_T)^2)^{1/2}} \quad (1)$$

at the middle work frequency where $\omega \tau_E \gg 1 > \omega \tau_T$ and

$$R_v = \frac{\eta p}{C \sum c_{vi} d_i} \frac{1}{\omega} \quad (2)$$

at high frequency where $\omega \tau_E \gg \omega \tau_T \gg 1$, where p is the pyroelectric coefficient of P(VDF-TrFE), k_T is the thermal conductance to the environment for per unit area of the detector, C is the sum of the capacitance of detector and amplifier of the measurement circuit, c_{vi} is the specific thermal capacity for the i th layers of the device. The summation \sum is taken over the layers the device consists of. Based on the measured pyroelectric coefficient ($27 \mu\text{C}/\text{m}^2\text{K}$), an average specific thermal capacity $2.4 \text{ J}/\text{cm}^3$ for the electrodes and P(VDF-TrFE), a thickness of 120 nm of the electrodes and the capacitance of detector (16 pF) and the amplifier (5 pF), the parameters extracted from the simulation are given in Table 1. As can be seen from the table, the first parameter η for Al/P(VDF-TrFE)/NiCr is 0.11, which is about three times larger than the counterpart value of 0.03 for Al/P(VDF-TrFE)/Al. This indicates better IR radiation absorbing performance of NiCr than Al films. The second parameter τ_T for Al/P(VDF-TrFE)/NiCr is 60 ms, which is smaller than the corresponding value of 110 ms.

Besides, it is noted that the third parameter k_T are similar for both structures. Thus, it can be simply concluded that better performance of detectors can be obtained with NiCr as absorption layer. However, comparing with ideal situation, where $k_T = 6.4 \times 10^{-3} \text{ W}/\text{cm}^2\text{K}$ and $\eta = 1$ ^[12], the performance of Al/P(VDF-TrFE)/NiCr detectors in our case can be further improved by optimizing these two parameters.

Tables 1 The parameters of free-standing detector with Al/P(VDF-TrFE)/NiCr and Al/P(VDF-TrFE)/Al structure

表1 Al/P(VDF-TrFE)/NiCr and Al/P(VDF-TrFE)/Al 探测器的参数

Simulated parameters	Al/P(VDF-TrFE)/NiCr	Al/P(VDF-TrFE)/Al
η	0.11	0.03
τ_T/ms	60	110
$k_T/(\text{W}/\text{cm}^2\text{K})$	2.5×10^{-3}	2.1×10^{-3}

To further study the absorbing behavior of Al/P(VDF-TrFE)/NiCr detectors, the reflectivity of a trilayer film with the same vertical structure was measured with an FTIR spectrometer. The absorption of the device was determined from $A = 1 - R - T$, where A is the absorption, R the reflection, and T is the transmission of the light. In our case, the bottom electrode is thick enough, so that $T = 0$. The result is shown in Fig. 4. The absorption of the device is not 50% as expected for a mono metal layer with a surface resistance matched to the vacuum impedance of incident light in the measured wavelength range^[8]. The interference of the lights reflected from the top and bottom electrodes at short wavelength can be observed. Thus the absorption of the sample can not be treated simply as a thin metal layer. At $6 \mu\text{m}$, the curve reads 70%. The diffusive scattering of the light caused by the roughness of the sample surface was omitted in the above consideration, resulting in an over estimated absorption value than the actual one, especially in the short wavelength, as compared with the value of $\eta = 0.1$ obtained from the fitting to experimental results.

With the above single element device, thermal image has been obtained via a two dimension scanning opti-

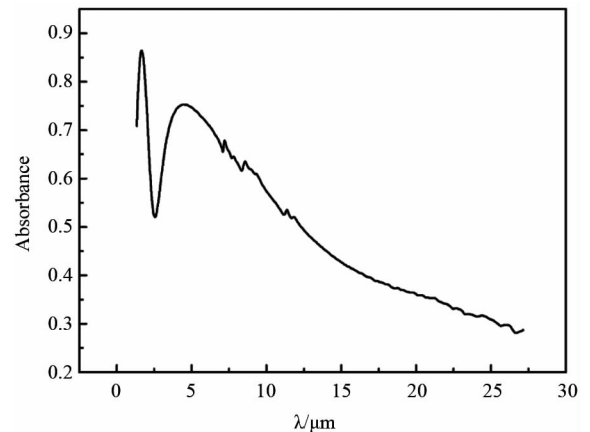


Fig. 4 Absorbance curve of Al/P(VDF-TrFE)/NiCr trilayers

图4 Al/P(VDF-TrFE)/NiCr 三层结构的吸收曲线

cal system. Figure 5 shows the thermal image of a target. The pigtail of the girl is distinct as can be seen from the figure. Despite of these unfavorable parameters $k_T = 2.5 \times 10^{-3} \text{ W/cm}^2\text{K}$ and $\eta = 0.11$, thermal image could be obtained benefiting from the high voltage responsibility. The performance of the detector can be further improved by increasing the absorption of the detector and decreasing the thickness of the P(VDF-TrFE), thus the thermal time constant of the device.

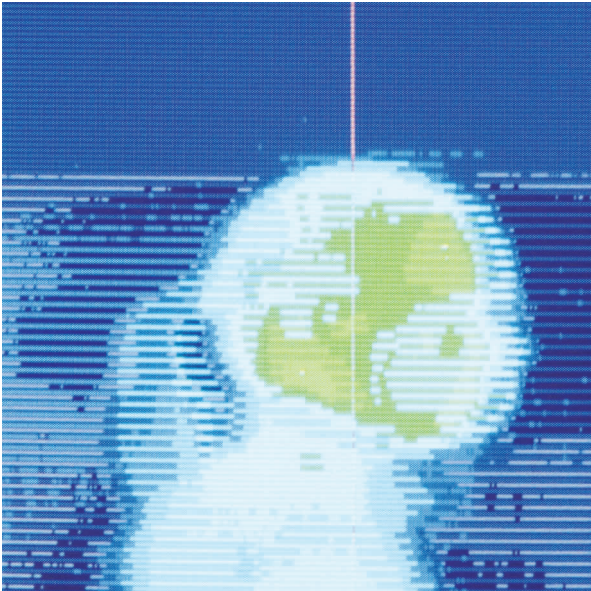


Fig5 IR image of a target with P(VDF-TrFE) detector
图5 采用P(VDF-TrFE)探测器实现的目标成像图

3 Conclusion

The fabricated P(VDF-TrFE) films have good ferroelectric and pyroelectric properties. Comparing with Al/P(VDF-TrFE)/Al detector, Al/P(VDF-TrFE)/NiCr sample exhibits better performance because of better NiCr absorbing behavior. The thermal conductance of unit area to the environment and absorption of Al/P(VDF-TrFE)/NiCr detector were $k_T = 2.5 \times 10^{-3} \text{ W/cm}^2\text{K}$ and $\eta = 0.11$. Despite of these unfavorable parameters, good

thermal image could still be obtained. In future work, study should be done to optimize these two parameters for further improving the performance of the detector.

Acknowledgements

A project supported by Scientific Research Fund of Hunan Provincial Education Department (Grant No. 14B041), the Natural Science Foundation of Hunan Province (Grant No. 2015JJ6024 and No. 14JJ6040), and National Natural Science Foundation of China (51502087).

References

- [1] Hu W C, Yang C R, Zhang W L, *et al.* Thermodynamic equilibrium model of pyroelectric polycrystalline thin films[J]. *Appl. Phys. Lett.*, 2007, **90**(15):152902-1-3.
- [2] Murali P. Micromachined infrared detectors based on pyroelectric thin films[J]. *Rep. Prog. Phys.*, 2011, **64**: 1339-1388.
- [3] Seifert A, Murali P, Setter N. High figure-of-merit porous $\text{Pb}_{1-x}\text{Ca}_x\text{TiO}_3$ thin films for pyroelectric applications [J]. *Appl. Phys. Lett.*, 1998, **72**(19):2409-2411.
- [4] Fulyigin V, Salley E, Vakhutinsky P, *et al.* Free-standing films of $\text{PbSc}_{0.5}\text{Ta}_{0.5}\text{O}_3$ for uncooled infrared detectors[J]. *Appl. Phys. Lett.*, 2001, **78**(3):365-367.
- [5] Dias C, Das-Gupta D K, Hinton Y, *et al.* Polymer/ceramic composites for piezoelectric sensors[J]. *Sensor Actuat. A - Phys.*, 1993, **37-38**:343-347.
- [6] Wang J L. Study on preparation and performance of ferroelectric polymer multilayer films [D]. Shanghai Institute of Technical Physics, Chinese Academy of Sciences, 2010.
- [7] Whatmore R W. Pyroelectric devices and materials[J]. *Rep. Prog. Phys.*, 1986, **49**:1335-1386.
- [8] Bauer S, Bauer-Gogonea S, Ploss B. The Physics of pyroelectric infrared devices[J]. *Appl. Phys. B-lasers o.* 1992, **54**:544-551.
- [9] Tian L. Study on fabrication and properties of ferroelectric polymer films[D]. Shanghai Institute of Technical Physics, Chinese Academy of Sciences, 2011.
- [10] Sharp E J, Garn L E. Use of low-frequency sinusoidal temperature waves to separate pyroelectric currents from nonpyroelectric currents. Part II. Experiment[J]. *J. Appl. Phys.*, 1982, **53**:8980-8987.
- [11] Fernandez M V, Suzuki A, Chiba A. Study of annealing effects on the structure of vinylidene fluoride-trifluoroethylene copolymers using WAXS and SAXS[J]. *Macromolecules*, 1987, **20**(8): 1806-1811.
- [12] Butler N R. Ambient temperature IR focal plane arrays[J]. *Proceedings of SPIE*, 2000, **4028**:58-65.